Experimental and Theoretical Studies on the Organic−Inorganic Hybrid Compound: Aluminum-NTCDA Co-Deposited Film

Hiroto Tachikawa*

Division of Molecular Chemistry, Graduate School of Engineering, Hokkaido University, Sapporo 060-8628, Japan

Hiroshi Kawabata

Venture Business Laboratory, Kyoto University, Sakyo-ku, Kyoto, 606-8501, Japan

Ryoji Miyamoto, Ken-ichi Nakayama, and Masaaki Yokoyama

Material and Life Science Faculty of Engineering, Osaka University, Suita, Osaka 565-0871, Japan

Received: August 24, 2004; In Final Form: November 1, 2004

Electronic absorption, Fourier transform-infrared (FT-IR), and electron spin resonance spectra of aluminum−naphthalene tetracarboxylic dianhydlide (Al−NTCDA) co-deposited film have been measured at room temperature, and hybrid density functional theory (DFT) calculations have been carried out in order to elucidate the electronic states for the ground and low-lying excited states of the complexes. After the interaction of NTCDA with Al atom, the new electronic transition bands were appeared at near-IR region. The C═O stretching modes of NTCDA are red-shifted by the interaction with Al. From the DFT calculations, it was found that the electronic state of the complex at the ground state is characterized by a slight charge-transfer state expressed by $(Al_4)^{\delta+}(NTCDA)^{\delta-}$. The binding of Al to NTCDA is strong. The C═O double-bond character of NTCDA is changed to C−O single-bond-like character by the strong interaction of Al to the C═O bond. This is the origin of the red-shift of the FT-IR spectrum. The electronic states of organic−inorganic hybrid material were discussed on the basis of theoretical results.

1. Introduction

Molecular devices have been widely used as semiconductor, electroluminescence (EL), and photoconductivity materials.[1,2] Metal−organic compounds, one of the organic−inorganic hybrid molecular devices, have attracted considerable attention over the past decade in view of their potential applications in electronic and optelectronic devices.[3−11]

Naphthalene tetracarboxylic dianhydlide (NTCDA) is one of the high-performance molecular devices utilized for photocurrent multiplications and organic semiconductors (Scheme 1). It is known that electron conductivity increases significantly by the doping of metal atoms. For example, electron conductivity of free NTCDA ($\sigma = 10^{-8}$ S/cm) is drastically changed to $\sigma = 10^{-5}$ S/cm (Mg) and $\sigma = 10^{-2}$ S/cm (In) doped by magnesium and indium atoms, respectively, indicating that the electron conductivity increases about 3−6 orders of magnitude by the doping of metal atoms.[4] This increase is remarkably large as an organic semiconductor. Although this is an interesting point in NTCDA, the mechanism of the electron conductivity and electronic states of NTCDA−metal system are not clearly understood. Furthermore, it is known that the polymer and molecules doped by alkali metal are easily degraded by air. However, NTCDA doped by metals is relatively stable in air. This is another interesting point for NTCDA. However, the reason the doped NTCDA is stable in air is scarcely known.

In previous works,[12−16] we investigated theoretically the structures and electronic states of 3,4,9,10-perylene-tetracarboxylicacid-dianhydride (PTCDA),[12] which is the similar molecular semiconductor to NTCDA, and its complexes with the indium atom. We suggested that the In atom can bind strongly to the carbonyl group of PTCDA. The binding energy is calculated to be 178 kJ/mol for each atom in In_4PTCDA. This energy is strong and is almost equivalent to a covalent bond. Also, we investigated mechanism of electron and hole conductivities in molecular devices, such as poly-vinylbiphenyl (PVB)[13] and polysilanes,[14,15] by means of ab initio DFT and ab initio molecular dynamics (MD) methods.[16] The origin of the conductivity was elucidated on the basis of theoretical results.

In the present study, we investigated experimentally and theoretically the ground and excited states of the Al−NTCDA complex in order to elucidate the electronic states of Al_4-NTCDA. As it is known, the electronic state at the excited state, especially the first excited state, strongly correlates to the electron conductivity in molecular devices. Therefore, elucida-

SCHEME 1

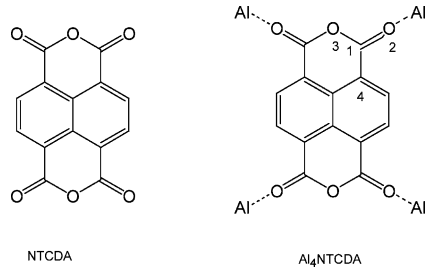

* Author to whom correspondence may be addressed. E-mail: hiroto@eng.hokudai.ac.jp. Fax.: +81 11706-7897.

10.1021/jp046168e CCC: $30.25
Published on Web 02/05/2005

tion of the electronic structures is important in development for new molecular devices. In the present study, we extend previous our techniques[12−16] to the molecular device $(Al)_n$-(NTCDA).

2. Methods

Experiments. NTCDA was supplied from Tokyo Kasei Kogyo and used after double purification by the train-sublimation technique. The co-deposited film of organic molecule and metal (Al−NTCDA) was prepared using separate sources at a pressure of 10^{-5} Torr. The concentration of metal was controlled by monitoring each deposition rate, which is typically 0.5 nm/s for organic and 0.02 nm/s for metal. The electrical conductivity was estimated from the current−voltage curve measured by a source-measure unit (Keithly, model 2400). The electronic characteristics of the Al−NTCDA co-deposited film are measured using a UV−vis spectrophotometer (JASCO, V570) and electronic spin resonance (ESR) spectrometer (Bruker, ESP-300). The film structures are evaluated using a Fourier transform infrared (FT-IR) spectrometer (Horiba, FT-720). The FT-IR spectra are measured using the attenuated total reflection (ATR) method. All the measurements were carried out under atmospheric conditions but immediately after deposition. Details of the experimental procedures are given in previous papers.[4,17]

Computational Calculations. All hybrid DFT calculations are carried out using Gaussian 98 program package.[18] The geometries of NTCDA and its complexes with aluminum atom $(Al)_n$(NTCDA) ($n = 4$) were fully optimized at the B3LYP/6-311++G(d,p) level of theory.[19] All calculations were carried out using 6-311++G(d,p) basis set. Harmonic vibrational frequencies for $n = 0$ and 4 were calculated for each optimized structure in order to check the stability of its geometry on the potential-energy surface. For $n = 1-3$, the structures were fixed to that of $n = 4$, and then Al atoms are removed from $(Al)_n$-(NTCDA). By use of the geometries, the excitation energies and oscillator strengths were calculated by means of time-dependent DFT calculations at the B3LYP/6-311++G(d,p) level. A total of 12 electronic excited states were solved for all species.

3. Results

A. UV−Vis, FT-IR, and ESR Measurements. Figure 1 shows the electronic absorption spectra of NTCDA and Al−NTCDA co-deposited films. NTCDA shows two peaks at $\lambda =$ 367 and 388 nm, which can be assigned to the symmetry-allowed $\pi-\pi^*$ transition. After the doping of aluminum atom to NTCDA, the spectrum of the NTCDA shows remarkable change: the original peaks of the $\pi-\pi^*$ transition decreased, and consequently four peaks at $\lambda =$ 430, 540, 700, and 1200 nm emerged. These peaks are consisted of broad bands.

FT-IR spectra of pure NTCDA and Al−NTCDA systems are given in Figure 2. The pure NTCDA film shows that a distinct peak at 1770 cm^{-1}, resulting from the C═O stretching mode and a peak at 1580 cm^{-1}, resulting from C−O stretching mode. Both peaks are weakened in the co-deposited film. Instead, four peaks are appeared at 1715, 1680, 1560, and 1515 cm^{-1}. The first two peaks are composed of broad bands around 1700 cm^{-1}.

ESR spectrum of co-deposited film Al−NTCDA is plotted in Figure 3. The symmetric line shape with no hyperfine structure is obtained at room temperature. The g value is obtained to be $g = 2.004$, which is slightly larger than that of free electron ($g_e = 2.0023$). Pure NTCDA films are inactive as the ESR spectrum. This result indicates that the co-deposited film Al−NTCDA includes at least a paramagnetic species. The

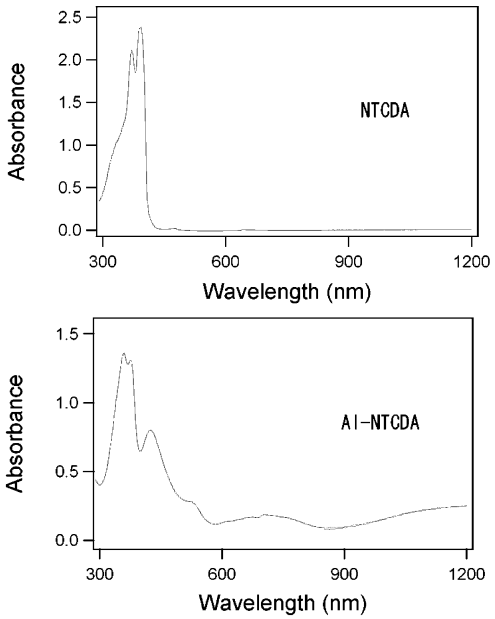

Figure 1. Absorption spectra of pure NTCDA (top) and Al−NTCDA co-deposited film (bottom).

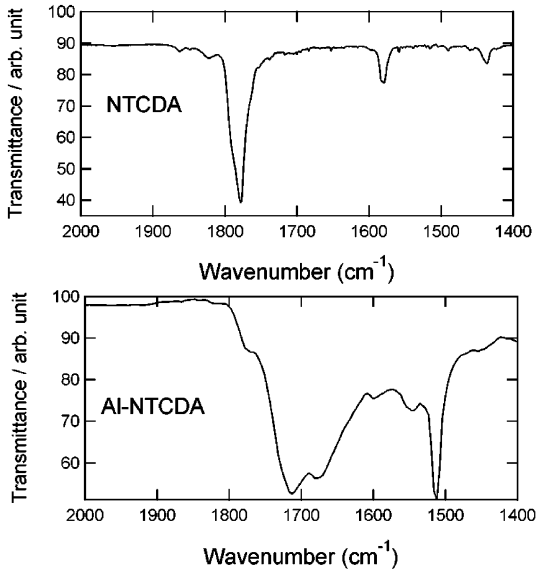

Figure 2. FT-IR spectra of pure NTCDA (top) and Al−NTCDA co-deposited film (bottom).

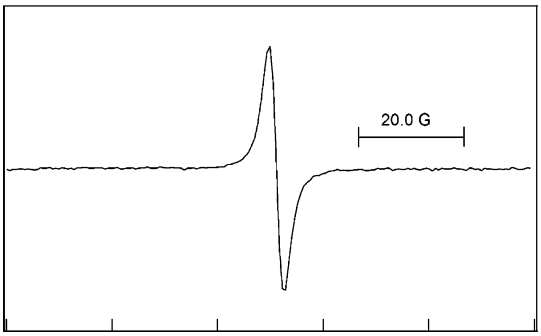

Figure 3. ESR spectrum of Al−NTCDA co-deposited film.

spin density of the radical was estimated to be 10^{-7} mol/L from the ESR spectrum.

The electrical conductivity of the Al−NTCDA film is measured to be 4.86×10^{-5} S/cm. This value is 2×10^3 times larger than that of pure NTCDA film (2.5×10^{-8} S/cm). For

TABLE 1: Selected Optimized Geometrical Parameters of Free NTCDA and $(Al)_4$(NTCDA) Calculated at B3LYP/6-311++G(d,p) Levels of Theory[a]

		$(Al)_4$NTCDA	
parameter	NTCDA	singlet	triplet
$C_1{=}O_2$	1.195	1.318	1.306
$r(O_2{-}Al)$		1.750	1.760
$\angle C_1{-}O_2{-}Al$		160.4	173.6

[a] Bond lengths and angles are in angstroms and degrees, respectively.

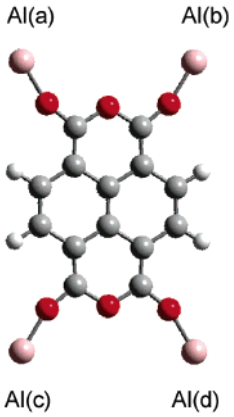

Figure 4. Optimized structure of $(Al)_4$(NTCDA) calculated at the B3LYP/6-311++G(d,p) level. Positions of Al atoms around NTCDA are shown in *a*, *b*, *c*, and *d*.

the other metals, the electrical conductivities were measured to be 1.3×10^{-2} S/cm for In/NTCDA, 1.2×10^{-5} S/cm for Ag/NTCDA, and 1.2×10^{-5} S/cm for Au/NTCDA.

The electrical conductivity of Al−NTCDA was changed as a function of time. This is due to the fact that the water or oxygen in air reacts with Al−NTCDA, and then the chemical structure is changed. In fact, the present measurement shows that the electrical conductivity of Al−NTCDA prepared in a vacuum is decreased after the condition under air. However, all spectra in the present study were measured immediately after the deposition. Hence, it is considered that the effects of atmosphere on the spectra are remarkably small.

B. DFT Calculations on the Structures of Al−NTCDA. The structure of free NTCDA is fully optimized at the B3LYP/6-311++G(d,p) level of theory. In the calculation, the molecular symmetry of NTCDA is assumed as a D_{2h} symmetry throughout. The results are given in Table 1. The C═O bond length is calculated to be $r(C_1{=}O_2) = 1.195$ Å. The distance between the oxygen and carbonyl carbon atoms is $r(C_1{-}O_3) = 1.389$ Å, while the C−C distance (denoted by $C_1{-}C_4$) is calculated to be 1.483 Å, which corresponds to a normal distance of the C−C single bond.

Next, the molecular complex composed of NTCDA and four aluminum atoms, expressed by $(Al)_n$(NTCDA) ($n = 4$), is optimized under the D_{2h} symmetry. The optimized structure obtained for the singlet state is given in Figure 4. The aluminum atom is located at a distance of 1.750 Å from the carbonyl oxygen atom of NTCDA ($r(O_2{-}Al)$). The angle of Al−O−C is calculated to be $\angle C_1{-}O_2{-}Al = 160.4°$, meaning that the Al−O−C bond is not linear. The interatomic distance between aluminum atoms (positions a and b in Figure 4) is calculated to be 6.307 Å, which is long enough to allow no interaction as through-space. The C═O bond distance in $(Al)_n$(NTCDA) ($n = 4$) is calculated to be $r(C_1{=}O_2) = 1.318$ Å, which is largely elongated from that of free NTCDA (1.195 Å). On the other hand, the C−C bond distance (denoted by $C_1{-}C_4$) is shortened from 1.483 to 1.358 Å by the interaction with aluminum atom. The double bond of C═O carbonyl of NTCDA becomes single-bond-like (C−O−Al) after the interaction with the Al atom.

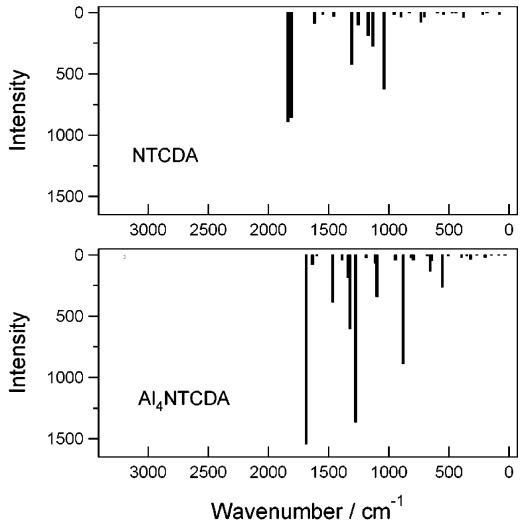

Figure 5. Harmonic vibrational frequencies of free NTCDA (upper) and Al_4NTCDA (lower) calculated at the at the B3LYP/6-311++G(d,p) level. The intensity of the IR band is in arbitrary units.

TABLE 2: Mulliken Atomic Charges on Al Atom and C═O Carbonyl Group Calculated at the B3LYP/6-311++G(d,p) Level

	NTCDA	$(Al)_4$NTCDA	
atom	singlet	singlet	triplet
Al		+0.17	+0.15
C	+0.10	+0.09	+0.15
O	−0.21	−0.08	−0.10

The structure of $(Al)_4$(NTCDA) at triplet state is optimized for comparison. The Al atom is located at 1.760 Å from the C═O carbonyl. The structure at the triplet state is significantly similar to that of singlet state.

As shown in Table 2, atomic charges of aluminum atom in Al_4NTCDA ($n = 4$) are +0.17, while NTCDA has a negative charge (−0.68) at the singlet state, indicating that the ground state of the complex is composed of a slight charge-separation character. For the triplet state, the similar electronic feature is obtained (the charge on Al atom is calculated to be +0.15).

To assign the FT-IT spectra obtained experimentally, harmonic vibrational frequencies of NTCDA and $(Al)_n$(NTCDA) ($n = 4$) are calculated. The vibrational frequencies and intensities for free NTCDA and complex $(Al)_n$(NTCDA) ($n = 4$) are illustrated in Figure 5. The calculations indicate that all frequencies are positive in both molecules, meaning that the optimized structures are located in the local minima. In free NTCDA, the frequencies are widely distributed in the range 30−3200 cm^{-1}. The higher two frequencies with negligible small intensities (3196 and 3178 cm^{-1}, each mode doubly degenerates) are assigned to the C−H stretching modes of the benzene rings of NTCDA. The frequencies calculated in middle region (1000−2000 cm^{-1}) are corresponding to C−C or C═O stretching modes. The peaks with the large intensities around 1800 cm^{-1} are assigned to be the C═O stretching modes of NTCDA. For example, the C═O stretching modes of NTCDA are calculated to be 1846 (a_g), 1838 (b_{1u}), 1809 (b_{3g}), and 1809 cm^{-1} (b_{2u}). These frequencies disappeared by the interaction with aluminum atom, as shown in Figure 5 (lower). Instead, new peaks are raised at 1638 (a_g), 1687 (b_{1u}), 1619 (b_{3g}), and 1596 cm^{-1} (b_{2u}). These new peaks are formed by the change

TABLE 3: Binding Energies (in kJ/mol) of Al to NTCDA Calculated at the B3LYP/6-311++G(d,p) Level[a]

Al atom	binding site	binding energy
$n = 1$	(a)	14.7
$n = 2$	(a,b)	297.6 (148.8)
	(a,c)	369.4 (184.5)
	(a,d)	349.8 (174.9)
$n = 3$	(a,b,c)	613.0 (204.3)
$n = 4$ (singlet)	(a,b,c,d)	871.5 (217.9)
$n = 4$ (triplet)	(a,b,c,d)	792.4 (198.1)

[a] The binding energies per one Al atom are given in parentheses.

TABLE 4: Excitation Energies (in eV) of the NTCDA and $(Al)_4$(NTCDA) Complexes Calculated Using the TD-DFT Method (B3LYP/6-311++G(d,p) Level)[a]

excited state	free NTCDA	$(Al)_4$(NTCDA)
1st	3.40 (0.257)	1.36 (0.00)
2nd	3.43 (0.00)	1.49 (0.00)
3rd	3.58 (0.00)	1.50 (0.00)
4th	3.78 (0.067)	1.62 (0.362)
5th	3.96 (0.00)	1.72 (0.00)
6th	4.21 (0.00)	1.73 (0.00)

[a] The intensities of the spectra (in arbitrary units) are given in parentheses.

of bonding nature from the C═O double-bond character to the C−O single-bond character. In addition to these frequencies, vibrational modes which the C═O stretching vibrations are contaminated are appeared at a lower-energy region: 1364 (a_g), 1322 (b_{1u}), 1253 (b_{3g}), and 1276 cm^{-1} (b_{2u}).

C. Binding Energies of the Aluminum Atom to NTCDA. As shown in the previous section, it is found that the aluminum atom is bound to the carbonyl oxygen of NTCDA. Four aluminum atoms can bind to one NTCDA molecule. The binding energies of the aluminum atoms are summarized in Table 3. The aluminum atom in the 1:1 complex of Al−NTCDA is bound to a carbonyl oxygen atom with a binding energy of 14.7 kJ/mol in the case of the 1:1 complex. In the case of two aluminum atoms (2:1 complex), there are three binding sites depending on its binding positions: (a,b), (a,c), and (a,d), where (x,y) means binding sites of aluminum atoms, x and y. The binding energies of (a,b), (a,c), and (a,d) sites per one aluminum atom are calculated to be 148.8, 184.5, and 174.9 kJ/ mol, respectively. These values in the 2:1 complexes are significantly larger than those of the 1:1 complex. In the 3:1 and 4:1 complexes, the binding energies for the one-aluminum atom are 204.3 and 217.9 kJ/mol, respectively. These results strongly indicate that the binding of aluminum atoms to NTCDA enhances the binding energy of aluminum atom.

For comparison, the binding energy for the triplet state of Al_4NTCDA is calculated. The value obtained is 198.1 kJ/mol (per one Al atom), which is slightly smaller than those of the singlet state (217.9 kJ/mol).

D. Excitation Energies of NTCDA and $(Al)_n$(NTCDA) (n = 4). The electronic structures for the excited states are determined by means of time-dependent (TD)-DFT methods. First, the excitation energies of free NTCDA (i.e., $n = 0$) are calculated, and the results are summarized in Table 4. The first and second excited states are constructed by $^1B_{1u}$ and $^1B_{2g}$ states, respectively, and the excitation energies are calculated to be 3.40 and 3.43 eV, respectively. The electronic transition from the ground to first excited state, $^1Ag \rightarrow {}^1B_{1u}$, is "symmetry allowed" with a large transition moment ($f = 0.257$), which is large enough to observe experimentally as a strong absorption band.

It should be noted that the first and second excitation energies are observed experimentally to be 3.20 and 3.40 eV, which are in good agreement with the present calculations (3.40 and 3.78 eV, respectively). The agreement implies that TD-DFT calculation at the B3LYP/6-311++G(d,p) level would give a reasonable feature for the excitation energy and electronic structure of the excited states in the NTCDA system.

For the 4:1 complex, $(Al)_4$(NTCDA), the excitation energies for low-lying excited (singlet) states are calculated to be 1.36, 1.49, 1.50, 1.62, 1.72, and 1.73 eV. The lowest "symmetry-allowed" electronic transition is calculated to be 1.62 eV whose oscillator strength is 0.362. This intensity is large enough to detect experimentally as a strong absorption band.

To assign the absorption band appearing at 1.62 eV, the natural orbital of Al−NTCDA is analyzed in detail. The highest occupied and lowest unoccupied molecular orbitals (denoted by HOMO and LUMO, respectively) are illustrated by the isosurface in Figure 6. In addition, the next LUMO is also illustrated (denoted by LUMO + 1). The orbitals HOMO, LUMO, and LUMO + 1 correspond to 94th, 95th, and 96th MOs of $(Al)_4$(NTCDA). The HOMO of the complex is mainly composed of LUMO of free NTCDA and π-orbital of aluminum atoms, indicating that the electron of Al is slightly diffused into the LUMO of free NTCDA. Hence the aluminum atom has a slight positive charge. On the other hand, the orbital is localized on aluminum atom in LUMO + 1.

The natural orbital for the excited state (the excitation energy is 1.62 eV) is approximately expressed by

$$\Phi = C_1\phi(\text{HOMO} \rightarrow \text{LUMO} + 1) + C_2\phi(\text{HOMO} \rightarrow \text{LUMO}) + \ldots \quad (1)$$

The largest coefficient for the excited state is $C_1 = 0.64$, while the other coefficients are smaller than 0.30, implying that the main configuration is the HOMO → LUMO + 1 transition. These results indicate that the "symmetry-allowed" electronic transition appearing at 1.62 eV is attributed to a charge-transfer (CT) band between the aluminum atom and the carbonyl group. Also, it is found that the transition is assigned to back-donation from NTCDA to Al. This state is the origin of the CT band.

To confirm this feature in more detail, singly excited configuration interaction calculation (SE−CI) with the LANL2DZ basis set is carried out for the first excited state of Al_4NTCDA. The charge on the Al atom is changed from +0.61 (ground state) to +0.21 (first excited state) and to +0.17 (second excited state) by the excitation, indicating that the charge transfer takes place after the electronic excitation.

The main configuration of the lowest excitation band (denoted by $^1Ag \rightarrow {}^1B_{3g}$; the excitation energy is 1.36 eV) is expressed by HOMO → LUMO. Figure 6 (middle) shows LUMO of $(Al)_4$-(NTCDA), which is composed mainly of pure LUMO of free NTCDA. Therefore, the lower electronic excitation is also one of the CT bands.

E. Simulated Absorption Spectra of Free NTCDA and $(Al)_n$(NTCDA) (n = 1−4). In this section, we predict absorption spectra of $(Al)_n$(NTCDA) ($n = 4$) on the basis of the present calculations. Simulated absorption spectra are illustrated in Figure 7. In the plots of simulations, the half width of the spectrum is assumed to be 0.005 eV.

For pure NTCDA, the peaks of the absorption spectrum are appeared at the ultraviolet region (3.40 and 3.78 eV). The lowest "symmetry-allowed" excitation band is assigned to be the HOMO−LUMO transition of NTCDA (3.40 eV).

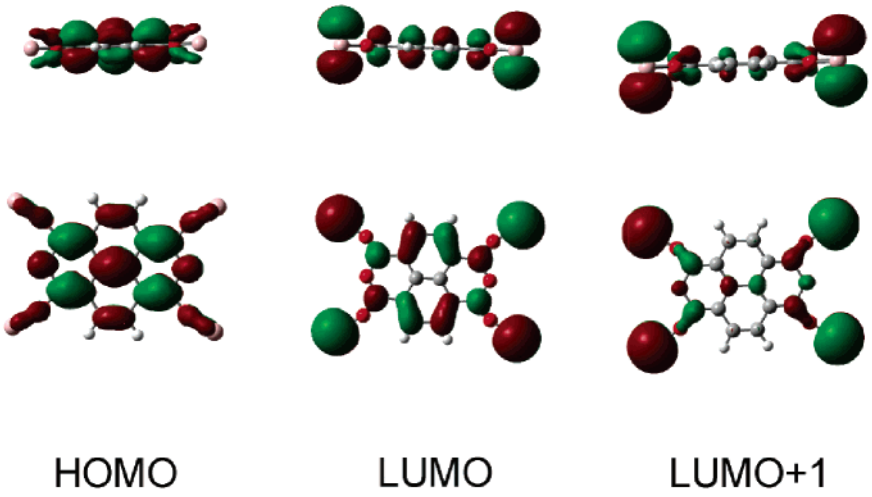

Figure 6. Illustrations of MOs of $(Al)_4$(NTCDA), HOMO, LUMO, and LUMO + 1, calculated at the B3LYP/6-311++G(d,p) level.

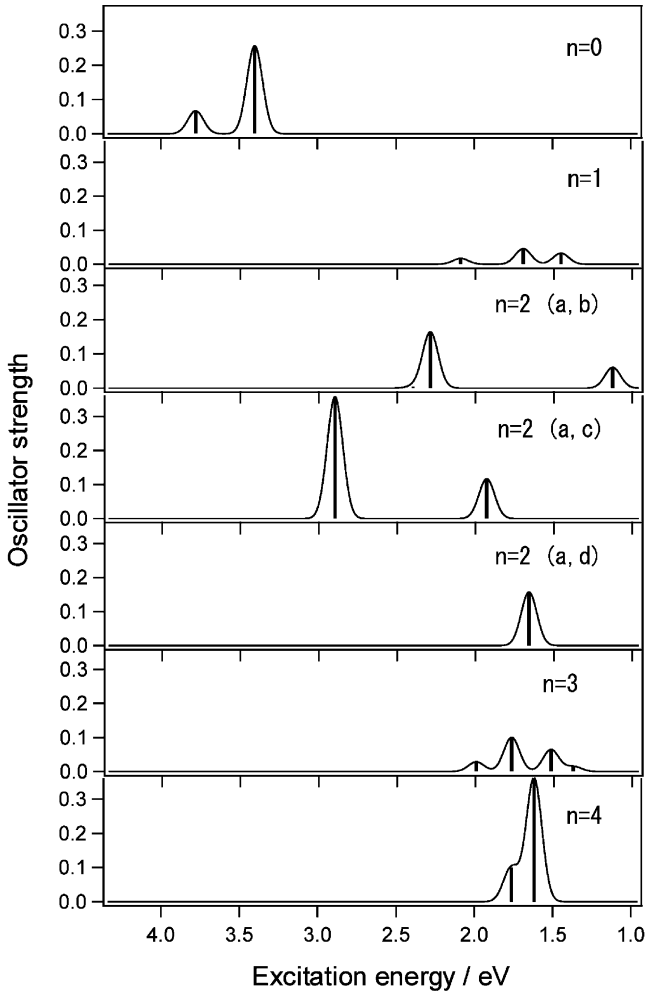

Figure 7. Simulated absorption spectra of $(Al)_n$(NTCDA) ($n = 0-4$) calculated at the B3LYP/6-311++G(d,p) level. Notation (m,n) means the position of aluminum atom around NTCDA (See, Figure 4). Relative oscillator strengths are in arbitrary unit.

For $n = 1$ and 3, the similar absorption spectra are obtained with each other: these are composed of three main peaks with small intensities. The lowest excitation energies are calculated to be 1.45 eV ($n = 1$) and 1.37 eV ($n = 3$), which are significantly lower than that of free NTCDA (3.40 eV). For $n = 2$, the absorption bands are widely distributed in the range 1.12−2.90 eV. The oscillator strengths for $n = 2$ are remarkably stronger than those of $n = 1$ and 3. For $n = 4$, the peak is located at 1.62 eV, and a strong intensity is obtained. This peak has a shoulder band at 1.70 eV.

Thus, it can be summarized that band structure of NTCDA is significantly changed by the interaction with aluminum atoms. The new energy bands are appeared at very low energy regions below 2.0 eV. In particular, it is predicted theoretically that new energy bands with a strong transition probability are generated around the excitation energies 1.5−2.0 eV in $n = 2$ and 4.

F. Spin Densities on $(Al)_n$(NTCDA) ($n = 1$ and 3). The NTCDA molecule has four hydrogen atoms in benzene rings. For the complex for $n = 1$, the hyperfine coupling constants of hydrogen atoms (H-hfcc's) of Al−NTCDA are calculated to be −4.79, −2.62, +1.25, and +0.61 G. In the case of $n = 3$, the H-hfcc's becomes smaller (−2.79, −0.06, +0.06, and +1.35 G). These results suggest that the H-hfcc's of $(Al)_n$(NTCDA) ($n = 1$ and 3) are significantly small. From these calculations, it is expected that the ESR spectrum of $(Al)_n$(NTCDA) ($n = 1$ and 3) shows a singlet line shape. This is in good agreement with the experiment.

G. Comparison with Experiments. Figure 8 shows the experimental absorption spectrum (solid curve) and theoretical values (stick diagram) of pure NTCDA and the Al−NTCDA systems. For pure NTCDA, theoretical calculation shows two peaks are appeared at 368 and 328 nm. These values are in qualitatively agreement with the experiments.

The experimental absorption spectrum of the Al−NTCDA co-deposited film and theoretical spectra of $(Al)_n$(NTCDA) ($n = 0-4$) are also given. From the comparison with the theoretical calculations, assignment of the absorption spectrum will be possible. The peak *a* consists of pure NTCDA with $n = 0$. The peaks *b*, *c*, and *e* are contributed from $n = 2$ (a,c), $n = 2$ (a,b), and $n = 2$ (a,b), respectively. The absorption peaks around 700 nm are composed of $n = 1$ and 3. From these theoretical calculations, it is strongly suggested that the experimental absorption spectrum of the Al−NTCDA co-deposited film is not composed of unique species, but the film consists of multicomponents such as $(Al)_n$(NTCDA) ($n = 0-4$).

In the present calculations, the complex $(Al)_n(NTCDA)_m$ ($n = 1-4$ and $m = 1$) was only considered. However, the possibility of other structures has also remained. To check this point, we preliminary calculate the complex $(Al)_n(NTCDA)_m$ ($n = 1$ and $m = 2$) at the B3LYP/LANL2MB level. The excitation energies for pure NTCDA, (Al)(NTCDA), and (Al)-$(NTCDA)_2$ were calculated to be 1.60, 1.46, and 0.77 eV,

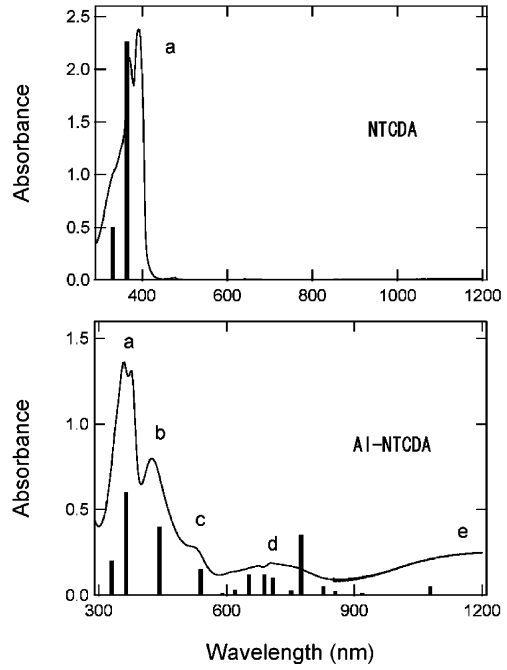

Figure 8. Experimental and theoretical absorption spectra of NTCDA (top) and Al−NTCDA (bottom) systems. (Solid curve) experimental spectra and (stick diagram) calculated values of $(Al)_n$(NTCDA) (n = 0−4). Intensity of absorption band is in arbitrary unit.

respectively. This result shows that the peak of the absorption appears in longer wavelength for the 1:2 complex. This shows that the broad band appearing at 1200 nm (peak *e*) may be composed of larger complexes $(Al)_n(NTCDA)_m$ (n = 1−2 and m = 2).

Discussion

A. Summary of the Present Study. In the present study, first, vis, FT-IR, and ESR spectra of pure NTCDA and Al−NTCDA co-deposited films were measured at room temperature. From these experiments, it is suggested that (1) the new excitation bands appear at near-IR regions after the interaction of NTCDA with Al, (2) the double-bond character of the C═O carbonyl of NTCDA is changed to a single-bond-like character after the interaction, and (3) the sample of co-deposited film Al−NTCDA includes at least one paramagnetic species.

Next, the hybrid DFT calculations have been applied to the molecular device $(Al)_n$(NTCDA) complexes (n = 0−4) in order to elucidate the electronic states of the complexes. From the calculations, it is found that the Al atom can bind to the carbonyl oxygen of NTCDA with a binding energy of 218 kJ/mol for one Al atom (B3LYP/6-311++G(d,p) level). The ground state of the complex for n = 4 is composed of a slight ionic character expressed by $(Al_4)^{\delta+}(NTCDA)^{\delta-}$, where the electron is somewhat transferred from aluminum to the carbonyl group. The magnitude of the charge transfer is estimated to be δ = 0.68. Thus, the solid of NTCDA behaves as a *n*-type semiconductor. This feature is the same as previous experiment.[4]

At the excited states, the electron is returned again to the Al atoms by the electronic excitation. From the MO characteristics, it is considered that the bonding nature between metal and the C═O carbonyl is changed to van der Waals interaction after the HOMO → LUMO + 1 transition. The change of electronic state can be schematically expressed by

$$(Al_4)^{\delta+}(NTCDA)^{\delta-} + h\nu \rightarrow (Al_4)(NTCDA)$$

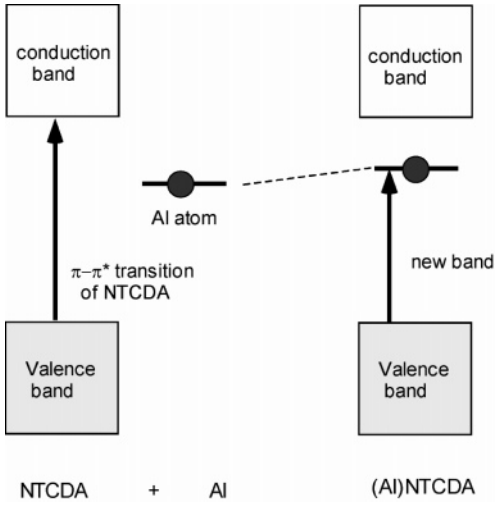

Figure 9. Model of band structures of the Al−NTCDA system proposed on the basis of the present study.

This electronic transition is the origin of the new band appearing at the near-IR region.

The calculations of harmonic vibrational frequencies of NTCDA and Al_4NTCDA complexes show that the peak of the C═O stretching mode of NTCDA is decreased by the interaction with Al atoms. Instead, the C−O single-bond-like mode is raised. This is due to the fact that the new bond is formed between C═O and Al. Hence, the spectrum of NTCDA is apparently red-shifted by the interaction. This feature is in good agreement with the present FT-IR experiment.

B. Doping Effects on the Electronic States. As mentioned in section 3D, it is found that new electronic bands are appeared by the interaction of NTCDA with aluminum atoms. On the basis of the present experimental and theoretical results, the mechanism of the interaction of NTCDA with Al atom is discussed here. A schematic illustration of the aluminum-doping effect to NTCDA film is given in Figure 9. The left side of Figure 9 indicates the schematic band structure of pure NTCDA film and energy level of free aluminum atom. The arrow indicates the electronic transition for the $\pi-\pi^*$ transition of NTCDA. If NTCDA interacts with aluminum (forming an Al−NTCDA co-deposited film), new bands appear at a low-energy region. The first "symmetry-allowed" electronic excitation is attributed to a charge-transfer band from NTCDA to aluminum atom. Thus, the present study indicates that the low-lying excited states appear as new energy states after the interaction of NTCDA with Al.

At the ground state, the electron is transferred from Al to NTCDA. Therefore, NTCDA possesses a negative charge. This indicates that the excess electron on NTCDA can easily move along the molecular sheets composed of NTCDA molecules. This is the origin of the electron conductivity in the molecular device of the Al−NTCDA system.

C. Comparison with Previous Studies. The metal−organic complexes of 3,4,9,10-perylene-tetracarboxylicacid-dianhydride (PTCDA), which is a very similar molecule to NTCDA, have been investigated from theoretical and experimental points of view.[4−11] In a previous paper,[16] we calculated energy bands of $(In)_n$(PTCDA) complexes (n = 1−4) using B3LYP and CI methods with a LANL2DZ base and suggested that the ground state is composed of an ion-pair state expressed by $(In_4)^{\delta+}$-$(PTCDA)^{\delta-}$. On the basis of MO characters, Kera et al. suggested that the new state of In_4(PTCDA)[10] is composed of a π state containing an In(5pz) orbital. The present calculations

for Al_4(NTCDA) showed the similar tendency for the electronic states at the ground state. However, the magnitude of the charge transfer from metal to the organic molecule in Al_4(NTCDA) is smaller than that of In_4PTCDA.

To clarify the properties of the organic/metal interface, Nakayama et al. investigated experimentally the electronic interaction between In and NTCDA using spectroscopic techniques.[4] The C═O and C−O stretching modes of NTCDA are measured to be 1770 and 1550 cm^{-1}, respectively. By the interaction with the In atom, the C═O stretching mode is red-shifted to be 1650 cm^{-1}. The present calculations showed that the C═O stretching mode of NTCDA is red-shifted by the interaction of C═O carbonyl with Al atom. This result indicates that the metal atoms (Al and In) bind to the C═O carbonyl of NTCDA. The present calculations predicted that the new energy band appears at the UV−vis region after the interaction of NTCDA with the metal atom. This feature is also observed for the Al−NTCDA system. These features also imply that the metal atoms interact with the C═O carbonyl of NTCDA.

An ion-pair state usually appears in the reaction of the carbonyl compounds with alkali metal atoms (M = Na and K).[20−25] For example, acetone−M and benzophenone−M complexes have been extensively investigated from theoretical and experimental points of view. From theoretical calculations,[20−26] it is suggested that the ground state of C═O−M moiety is an ion-pair state expressed by $C{=}O^{\delta-}\cdot\cdot M^{\delta+}$. On the other hand, the first excited state is composed of a van der Waals interaction expressed by C═O·M. This feature is verys similar to that of Al−NTCDA and In−PTCDA systems. This would be nature of bonding between the carbonyl compounds and metal atoms.

D. Additional Comments. We have introduced several approximations to calculate the structures and electronic states of the complexes. First, we used time-dependent DFT calculations to obtain the electronic states at the excited states. This method is convenient to obtain the excited states. However, description of the charge-transfer state is slightly underestimated. Therefore, more accurate wave function would be required to obtain more accurate excitation energies and charge distribution. It should be noted that the model presented here is effective in qualitative discussion. Second, we used a 6-311++G(d,p) basis set throughout the DFT calculations. To obtain more detailed features for the ion-pair state, one may need a variety of basis sets. Such calculations will be possible after development of a high-speed CPU in near future. Despite the several assumptions introduced here, the results enable us to obtain valuable information on the electronic states of the Al−NTCDA systems.

Acknowledgment. The authors are indebted to the Computer Center at the Institute for Molecular Science for the use of the computing facilities. One of the authors (H.T.) also acknowledges partial support from a Grant-in-Aid for Scientific Research from the Japan Society for the Promotion of Science.

References and Notes

(1) Katz, H. E.; Lovinger, A. J.; Johnson, J.; Kloc, C.; Li, W.; Lin, Y.-Y.; Dodabalapur, A. *Nature* **2000**, *404*, 478.

(2) Burroughes, J. H.; Jones, C. A.; Friend, R. H. *Nature* **1988**, *335*, 137.

(3) Forrest, S. R. *Chem. Rev.* **1997**, *97*, 1793 and references therein.

(4) Nakayama, K.; Niguma, Y.; Matsui, Y.; Yokoyama, M. *J. Appl. Phys.* **2003**, *94*, 3216.

(5) Greenham, N. C.; Friend, R. H. *Sold State Phys.* **1995**, *49*, 1.

(6) Azuma, Y.; Iwasaki, K.; Kurihara, T.; Okudaira, K. K.; Ueno, N. *J. Appl. Phys.* **2002**, *91*, 5024.

(7) Hirose, Y.; Chen, W.; Haskal, E. I.; Forrest, S. R.; Kahn, A. *Appl. Phys. Lett.* **1994**, *64*, 3482.

(8) Hirose, Y.; Kahn, A.; Aristiv, V.; Soukiassian, P.; Bulovic, V.; Forrest, S. R. *Phys. Rev. B* **1996**, *54*, 13748.

(9) Azuma, Y.; Akatsuka, S.; Okudaira, K. K.; Harada, Y.; Ueno, N. *J. Appl. Phys.* **2000**, *87*, 766.

(10) Kera, S.; Setoyama, H.; Onoue, M.; Okudaira, K. K.; Harada, Y.; Ueno, N. *Phys. Rev. B* **2001**, *63*, 115204.

(11) Palma, A.; Pasquarello, A.; Car, R. *Phys. Rev. B* **2002**, *65*, 155314.

(12) Tachikawa, H.; Kawabata, H. *J. Mater. Chem.* **2003**, *13*, 1293.

(13) Tachikawa, H.; Kawabata, H. *J. Phys. Chem. B* **2003**, *107*, 1113.

(14) Tachikawa, H. *J. Phys. Chem. A* **1999**, *103*, 2501.

(15) Tachikawa, H.; Yamada, Y.; Iyama, T. *J. Photochem. Photobiol. A* **1999**, *122*, 145.

(16) Tachikawa, H. *J. Phys. Chem. A* **2003**, *106*, 6915.

(17) Nakayama, K.; Niguma, Y.; Matsui, Y.; Yokoyama, M. *Jpn. J. Appl. Phys.* **2003**, *42*, L1478.

(18) Ab initio MO. Frisch, M. J.; Trucks, G. W.; Schlegel, H. B.; Scuseria, G. E.; Robb, M. A.; Cheeseman, J. R.; Zakrzewski, V. G.; Montgomery, J. A., Jr.; Stratmann, R. E.; Burant, J. C.; Dapprich, S.; Millam, J. M.; Daniels, A. D.; Kudin, K. N.; Strain, M. C.; Farkas, O.; Tomasi, J.; Barone, V.; Cossi, M.; Cammi, R.; Mennucci, B.; Pomelli, C.; Adamo, C.; Clifford, S.; Ochterski, J.; Petersson, G. A.; Ayala, P. Y.; Cui, Q.; Morokuma, K.; Malick, D. K.; Rabuck, A. D.; Raghavachari, K.; Foresman, J. B.; Cioslowski, J.; Ortiz, J. V.; Stefanov, B. B.; Liu, G.; Liashenko, A.; Piskorz, P.; Komaromi, I.; Gomperts, R.; Martin, R. L.; Fox, D. J.; Keith, T.; Al-Laham, M. A.; Peng, C. Y.; Nanayakkara, A.; Gonzalez, C.; Challacombe, M.; Gill, P. M. W.; Johnson, B. G.; Chen, W.; Wong, M. W.; Andres, J. L.; Head-Gordon, M.; Replogle, E. S.; Pople, J. A. *Gaussian 98*, revision A.5; Gaussian, Inc.: Pittsburgh, PA, 1998.

(19) Becke, A. D. *J. Chem. Phys.* **2003**, *98*, 5648.

(20) Tachikawa, H.; Murai, H.; Yoshida, H. *J. Chem. Soc., Faraday Trans.* **1993**, *89*, 2369.

(21) Wang, L. T, Su, T. M. *J. Phys. Chem. A* **2000**, *104*, 10829.

(22) Tsunoyama, H.; Ohshimo, K.; Yamakita, Y.; Misaizu, F.; Ohno, K.; *Chem. Phys. Lett.* **2000**, *316*, 442.

(23) Kaiser, E. T.; Levan, L. In *Radical Ions*; Interscience: New York, 1968.

(24) Davis, A. G.; Neville, A. G. *J. Chem. Soc., Perkin Trans.* **1992**, *2*, 169.

(25) Kawabata, H.; Tachikawa, H. *Phys. Chem. Chem. Phys.* **2003**, *5*, 3587.

(26) Tachikawa, H. *J. Phys. Chem. A* **2004**, *108*, 7853.